Electronic Supplementary Information (ESI)

Elastic sandwich-type GaN/MnO_2/MnON composites for flexible supercapacitors with high energy density

Shouzhi Wang[1], Yongliang Shao[1], Weikang Liu[2], Yongzhong Wu[1], Xiaopeng Hao[1]*

1. State Key Lab of Crystal Materials, Shandong University, Jinan, 250100, P.R. China
2. School of Physics, Shandong University, Jinan, 250100, P.R. China

*e-mail: xphao@sdu.edu.cn

This file includes:

S1. Materials

KOH, $KMnO_4$ PVA, Urea, and Ga_2O_3 were purchased from Sinopharm Chemical Reagent Co., Ltd. (Shanghai). NH_3, N_2 purchased from Deyang special Gas Co., Ltd. (Jinan, China).

S2. Characterization Methods

XRD was collected by a Bruker D8 Advance X-ray diffractometer with Cu Kα radiation (λ = 1.5406 Å). Raman spectra of samples were obtained with a LabRAM HR system of Horiba Jobin Yvon at room temperature and using a 532 nm solid state laser as the excitation source. Scanning electron microscopy (SEM) images were obtained using a Hitachi S-4800 field emission microscope. Energy-dispersive spectroscopy (EDS) elemental scans were performed on the same instrument equipped with a detector (7593-H, Horiba).High-resolution transmission electron microscopy (HRTEM) images were obtained on a Philips Tecnai Twin-20U high-resolution transmission electron microscope that operates at an accelerating voltage of 200 kV.

The surface area was determined by Brunauer–Emmett–Teller (BET) measurements with an ASAP 2020 sorptometer. PSD was determined according to Barrett–Joyner–Halenda (BJH) desorption dV/dlog(r) plot. Fourier transform infrared (FT-IR) spectra were collected on a Shimadzu IR Prestige-21 infrared spectrometer using pressed KBr discs. AFM images were obtained using a Nanoscope Multi Mode V (Digital Instruments/Bruker Systems), operating in ScanAsyst Airmode.

S3.Electrical conductivity tests

To measurement the conductivity of the samples, GaN/MnO_2/MnON were cut into fibrous powder and dispersed in DI water by a sonication process. The mixture was then dropped onto Si substrate with a 300-nm-thick SiO_2 layer. Prior to the photolithography process, the SiO_2/Si substrate was cleaned by dilute hydrofluoric acid (HF), dilute hydrochloric acid (HCl), ethanol and deionized water. A typical photolithography process was used to print electrodes on top of the respective fibers.

Electrical contacts to the GaN/MnO_2/MnON were made by defining source-drain electrodes separated by ~1000 nm with lithography technology (SUSS MicroTec

MBJ4) and subsequent evaporation of 50 nm Ti and 50 nm Au. Rapid thermal annealing was carried out at 500 °C for 3 min in the forming gas (10% H_2 in He) to improve the contact and passivate Si-SiO_x interface traps.1 The Ti/Au (30/50 nm) electrodes can maintain a good contact interface with an individual nanowire.

S4. Electrochemical Tests

All the electrochemical measurements with galvanostatic charge/discharge (GCD), cyclic voltammetry (CV), and electrochemical impedance spectroscopy (EIS) techniques were conducted using an electrochemical work-station (CHI660E). The electrochemical studies of single electrodes were performed in a three-electrode configuration, with a platinum sheet (1 cm × 1 cm) counter-electrode, Hg/HgO and Ag/AgCl as reference electrode, in 6.0 M KOH and 1M Na_2SO_4 aqueous solution.

For detail, CV and GCD curves were collected at −0.7 V to 0.3 V against Hg/HgO for the three-electrode system and 0–1.0 V for the two-electrode system by varying the scan rate from 1 mV s^{-1} to 200 mV s^{-1} and current density from 0.1 mA $cm^{-2}$to 20 mA cm^{-2}, respectively. Alternating current EIS spectra were collected within a frequency range of 10^{-2} Hz–10^5 Hz at the open circuit voltage with AC amplitude of 5 mV.

For three-electrode cells, areal capacitance (C_a) derived from areal discharge curves was calculated as[2-4]

$$C_a = \frac{I\Delta t}{S\Delta V} \quad (1)$$

Where C_a is the areal capacitance (F cm^{-2}),I is the constant discharge current (A), Δt is the discharge time (s), ΔV is the voltage window (V), and S is the area of the working electrode (cm^2).

The specific capacities (Cs, mAh cm^{-2}) of the samples were calculated from the GCD curves based on the following equation:

$$C_s = \frac{I\Delta t}{3.6S} \quad (1)$$

where I (A) represents the discharge current, Δt (s) refers to the discharge time, and S (cm^2) corresponds to the area of the working electrode loading active materials.

For the flexible symmetric SCs, the capacitance for a single electrode (C_{single}) was calculated according to [5,6]

$$C_{single} = \frac{4I\Delta t}{S\Delta V} \quad (2)$$

where s is the total area of active material on the two electrodes (cm^2).

The capacitance for the measured supercapacitor cell (C_{cell}) was calculated as[4,7]

$$C_{cell} = \frac{I\Delta t}{S\Delta V} \quad (3)$$

where s is the total area of the active material on the two electrodes (cm^2).

The volumetric capacitance (C_v) derived from areal capacitance was calculated according to[8]

$$C_v = \frac{C_a}{V_a} \quad (4)$$

where C_v is the volumetric capacitance (F cm^{-3}), C_a is the areal capacitance (F cm^{-2}), and V_a is the volume of the SCs (per cm^2); here, V_a is approximately 0.05 cm^{-3}.

C_a derived from CVs was calculated according to[2, 3]

$$C_a = \frac{1}{sv(V_b - V_a)} \int_{V_a}^{V_b} I \mathrm{d}V \quad (5)$$

where $s$is the area of active material on the working electrode (cm^2), v is the scan rate (V s^{-1}), I is the discharge current (A), and V_b and V_a are the high- and low-voltage limits of the CV curves (V).

The energy density (E) and power density (P) of the supercapacitor cell were estimated according to Equations 5 and 6, respectively, given by[2-3]

$$E = \frac{C_{cell}\Delta V^2}{2} \quad (6)$$

$$P = \frac{E}{\Delta t} \quad (7)$$

where ΔV is the cell-operation voltage window (V) and Δt is the discharge time (h).

The electrical conductivity (κ) of the CF/GaN/MnO2 was calculated according to[9,10]

$$\kappa = \frac{l}{RA} \quad (8)$$

where l is theeffective length (m) of the fiber, R is the resistance (Ω) measured by I-V curves, and A is theeffectivesectional area (m^2) of the CF/GaN/MnO_2.

S5. Calculation of capacitance contribution

According to Dunn et. al.,[11] we explain the calculation details of capacitance contribution differentiation based on the CV curves as follows. First, the current against scan speed be expressed in the equation:

$$i = av^b \quad (9)$$

where i is the measured current under certain voltage, v is the sweep rate, a and b are adjustable parameters. When b equals 1, the current is fully contributed by capacitive behavior; When b equals 0.5, the current is fully ion-diffusion controlled contribution.

The b value can be obtained by plotting current and sweep rate in logarithm, namely, the gradient of linear plots.[12]

$$\log i = b \log v + \log a \quad (10)$$

In reality, the current can originate from both aforementioned contributions. Therefore, the b value can vary between 0.5 and 1. Taking that into consideration, we can rewrite Equation (1) so that the current is a sum of two parts: capacitive current (viz., b=1) and ion-diffusion controlled one (viz., b=0.5):[13]

$$i(V) = k_1 v + k_2 v^{1/2} \quad (11)$$

We are interested in the percentage of the capacitive current. So, in order to determine the $k1$ value, equation (3) can be reformulated as: [14]

$$i(V)/v^{1/2} = k_1 v^{1/2} + k_2 \quad (12)$$

Obviously, with a series test of CV curves under different scan speed, the $k1$ value can be determined from the linear plots of $i(V)/ v^{1/2}$ vs $v^{1/2.}$

S6. Supplementary Figures S1–S22

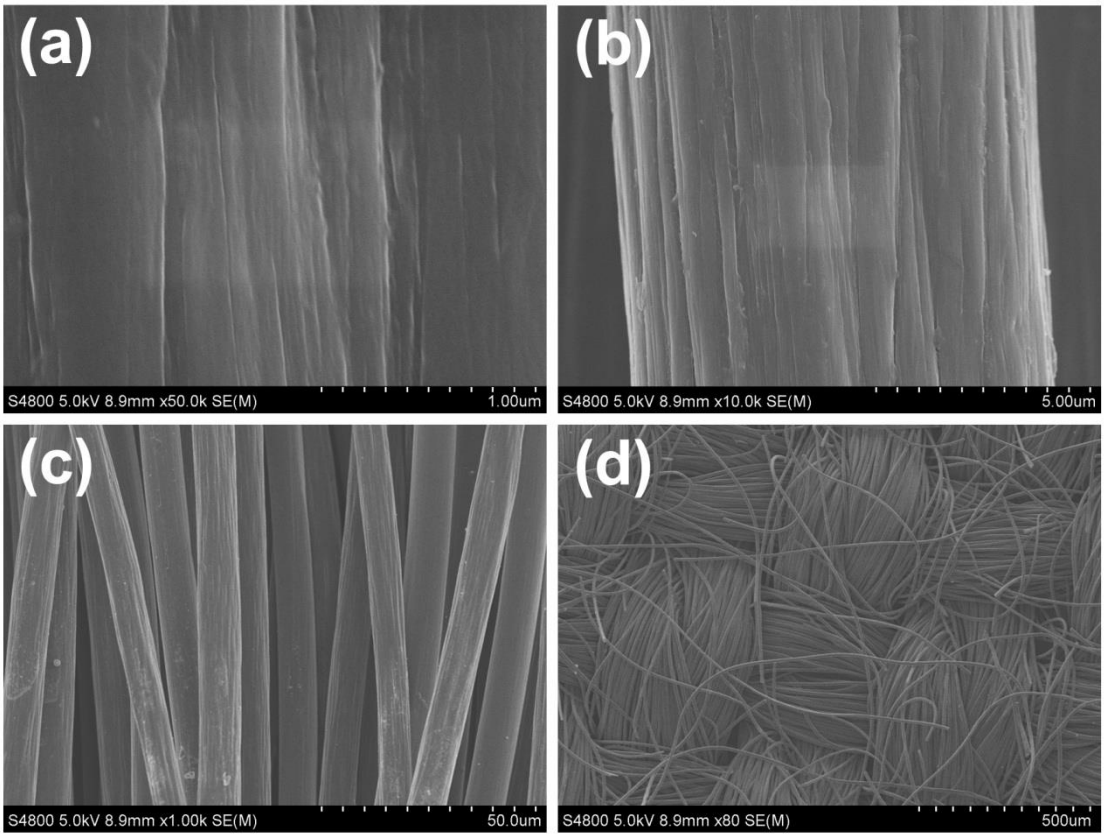

Figure S1.SEM images of CF at different magnification.

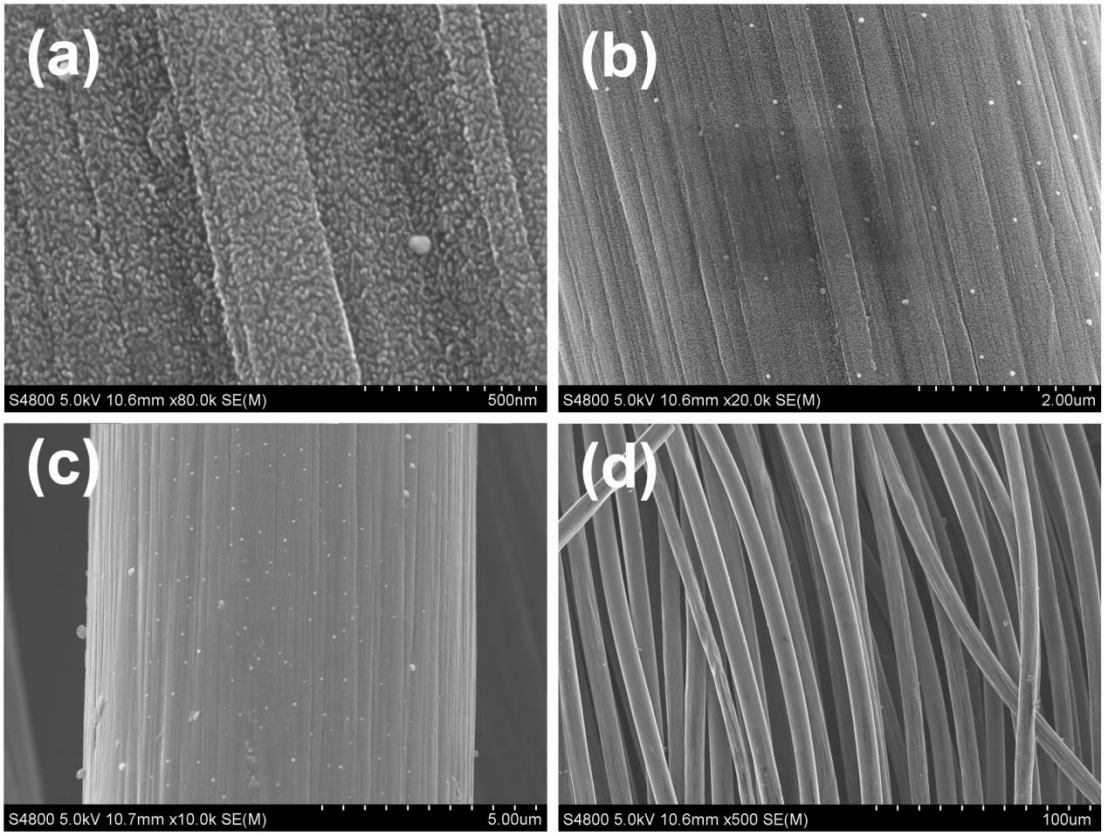

Figure S2.SEM images of CF treated by plasma at different magnification.

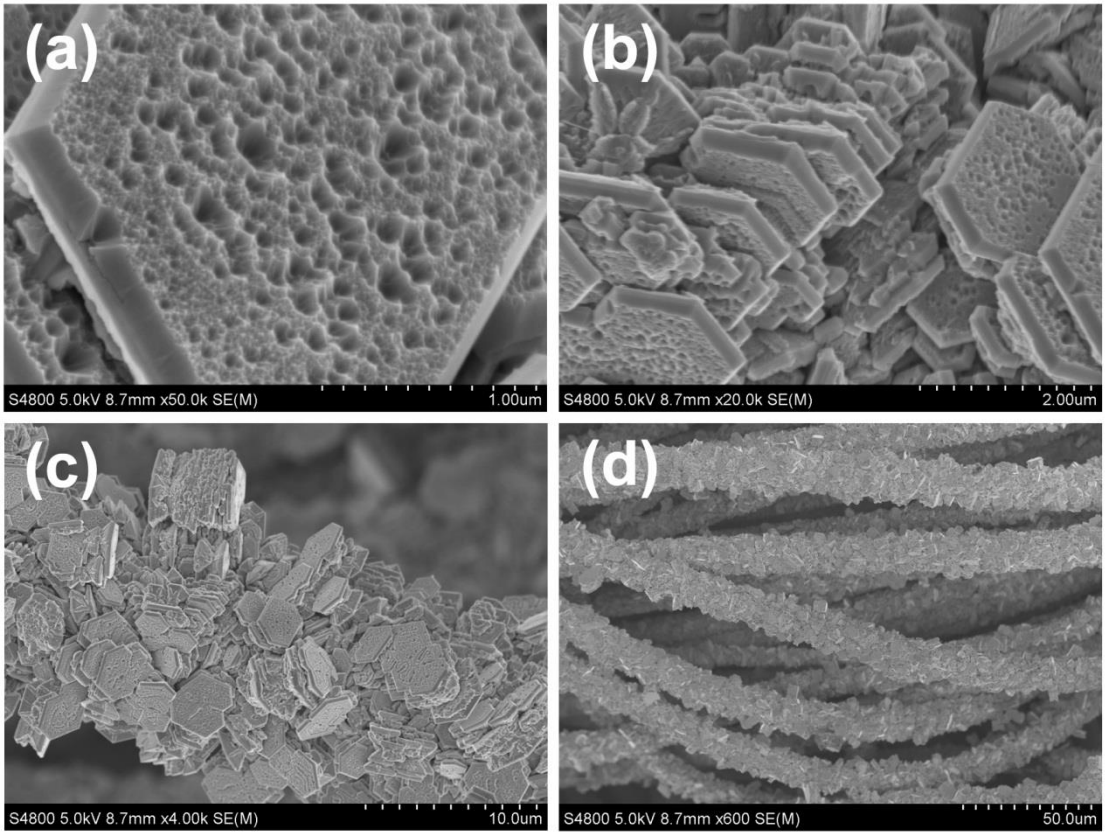

Figure S3.SEM images of the GaN nanocomposites at different magnification.

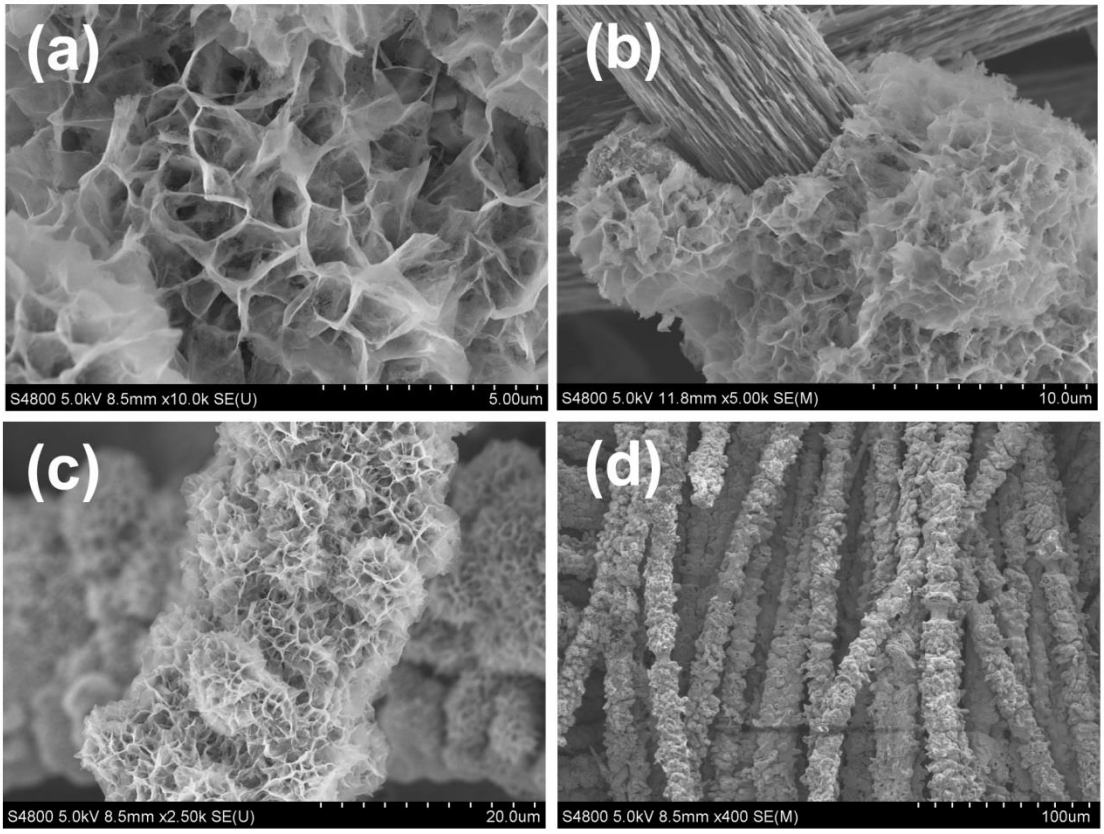

Figure S4. SEM images of the GaN/MnO_2/MnON nanocomposite under different magnification (a, c and d) and the cross-sectional view (b).

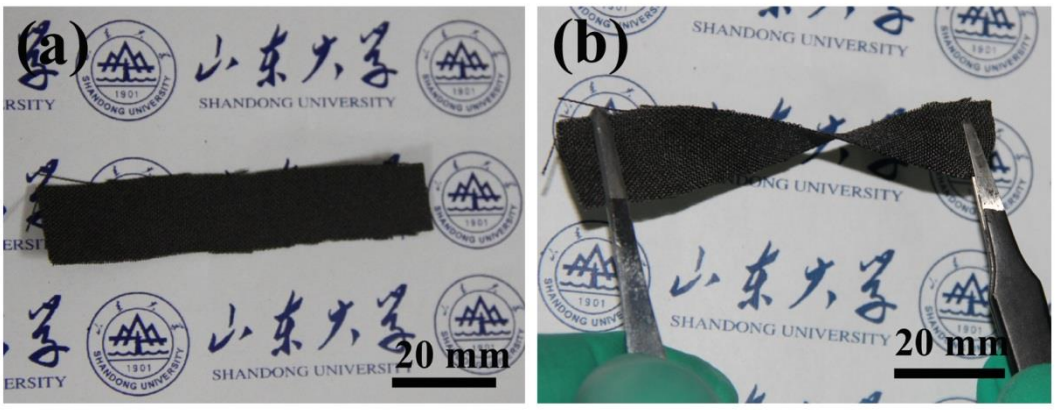

Figure S5. Photos of GaN/MnO_2/MnON (a) and show good flexibility (b).

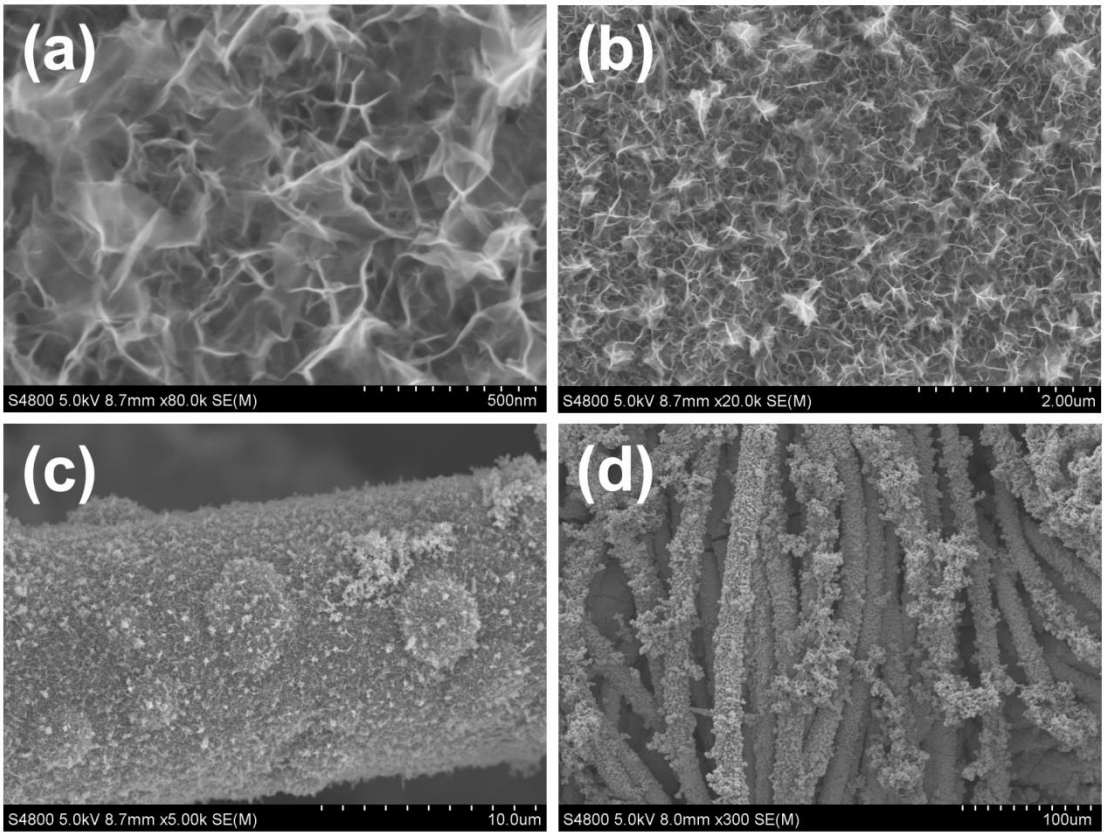

Figure S6. SEM images of the MnO_2 nanocomposite at different magnification.

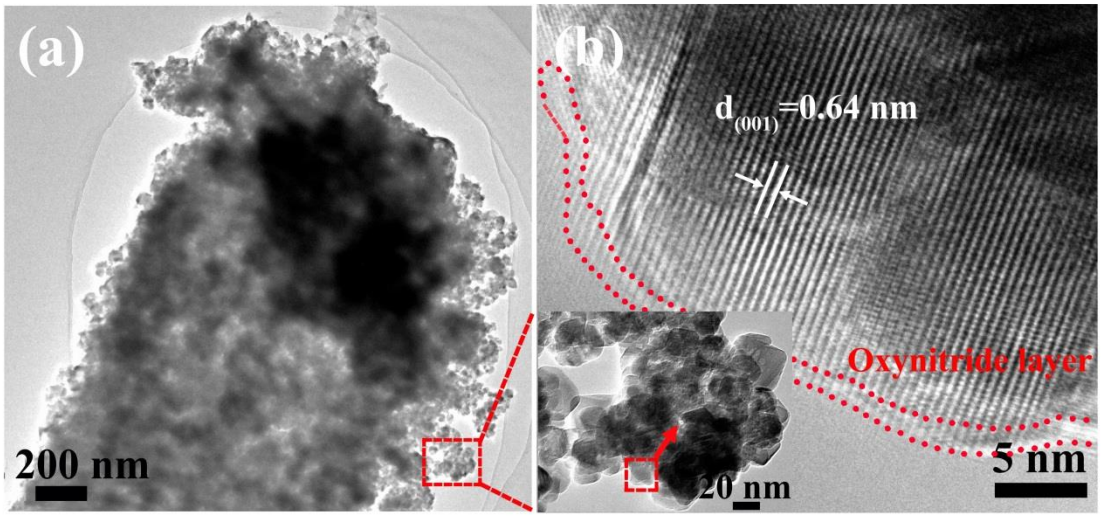

Figure S7. TEM images of the GaN/MnO_2/MnON nanocomposite at different magnification.

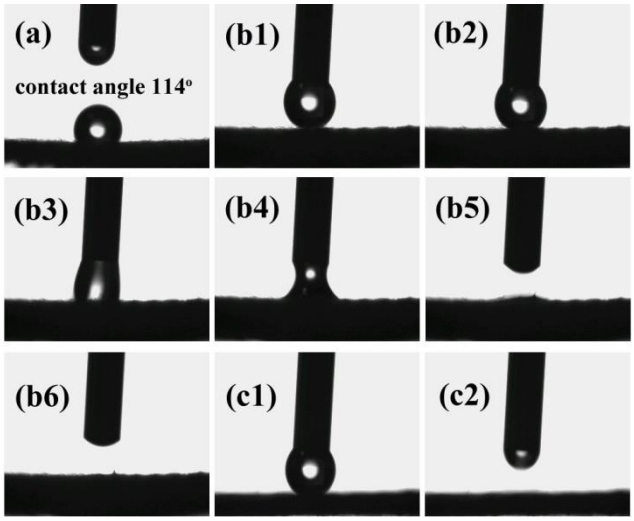

Figure S8. Water contact angles of CF (a), plasma treated CF (b1−b6) and GaN/MnO_2/MnON (c-1−c-2), each frame 1/24 s interval from b1 to b6 and c1 to c2.

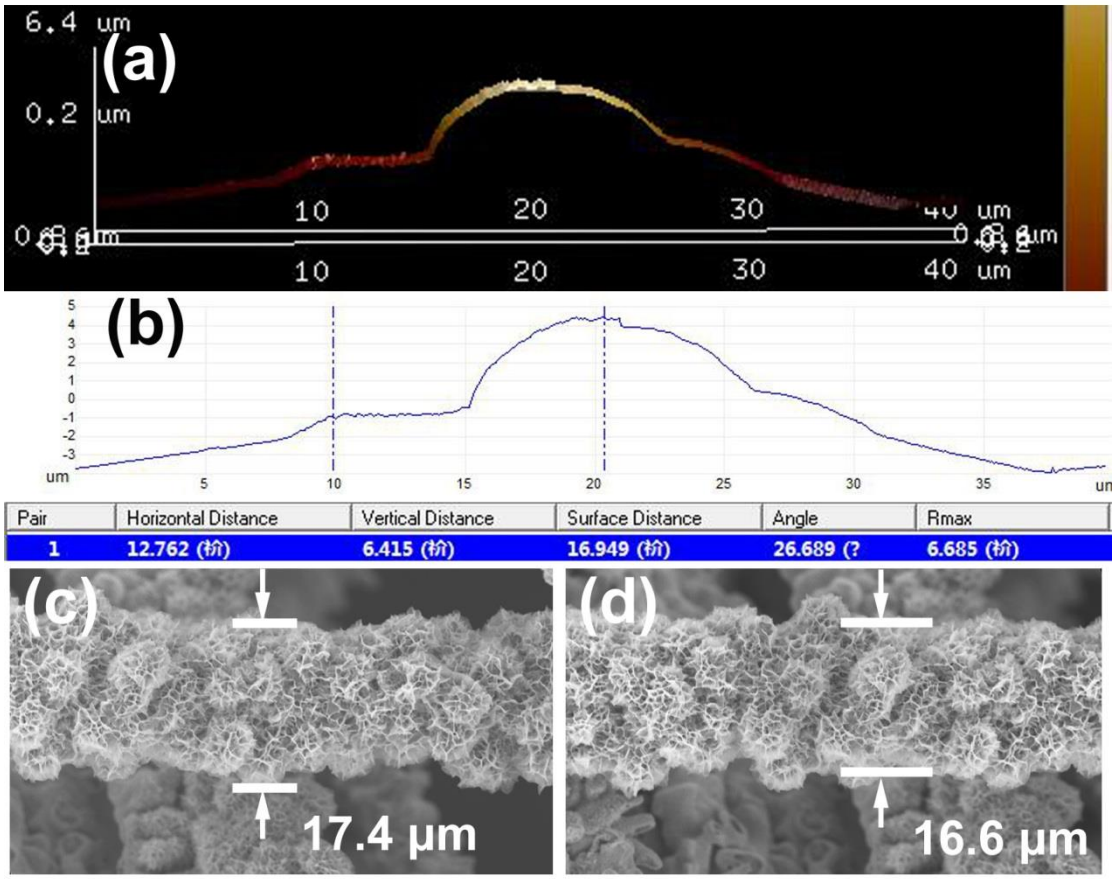

Figure S9. The diameter measurementof GaN/MnO_2/MnON composites: AFM (a-b) and SEM (c-d) characterization.

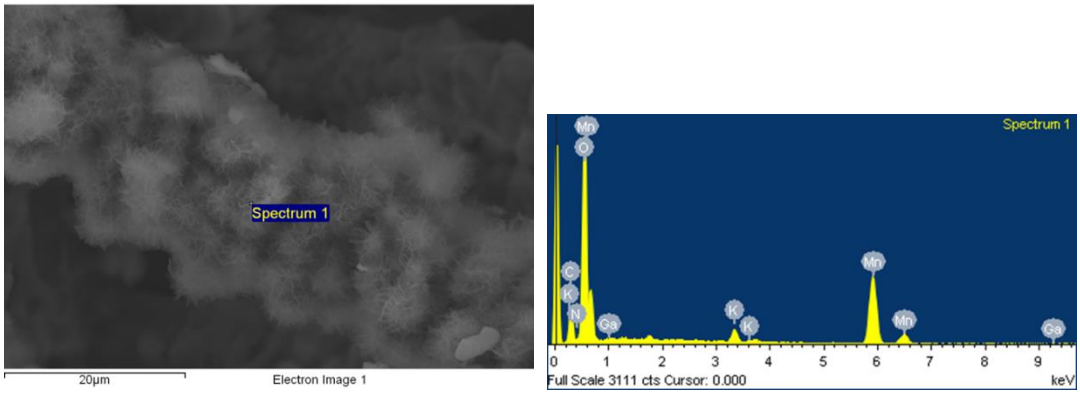

Figure S10. SEM image and EDS spectrum of GaN/MnO_2/MnON nanocomposite.

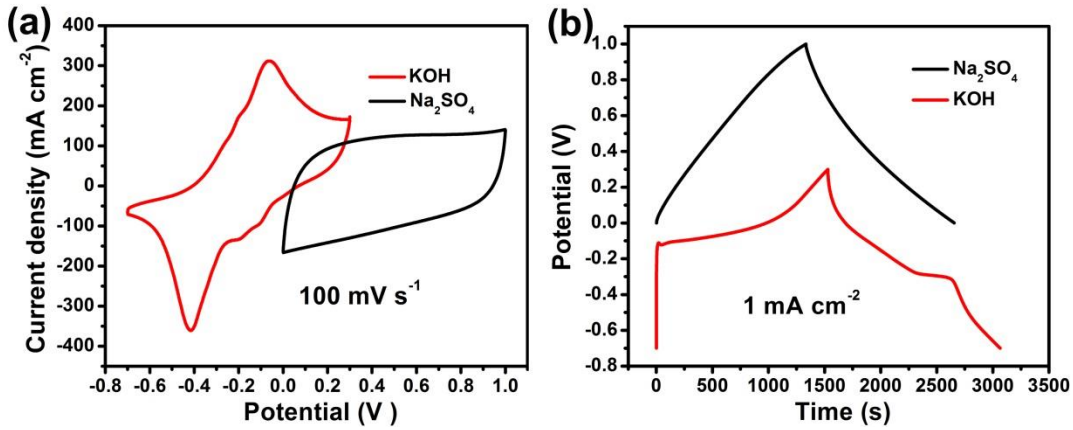

Figure S11. Comparisons of CV curves (a) at 100 mV s^{-1} and GCD curves (b) at 1 mA cm^{-2} of GaN/MnO_2/MnON electrode measured in 6 M KOH and 1 M Na_2SO_4 electrolyte, respectively.

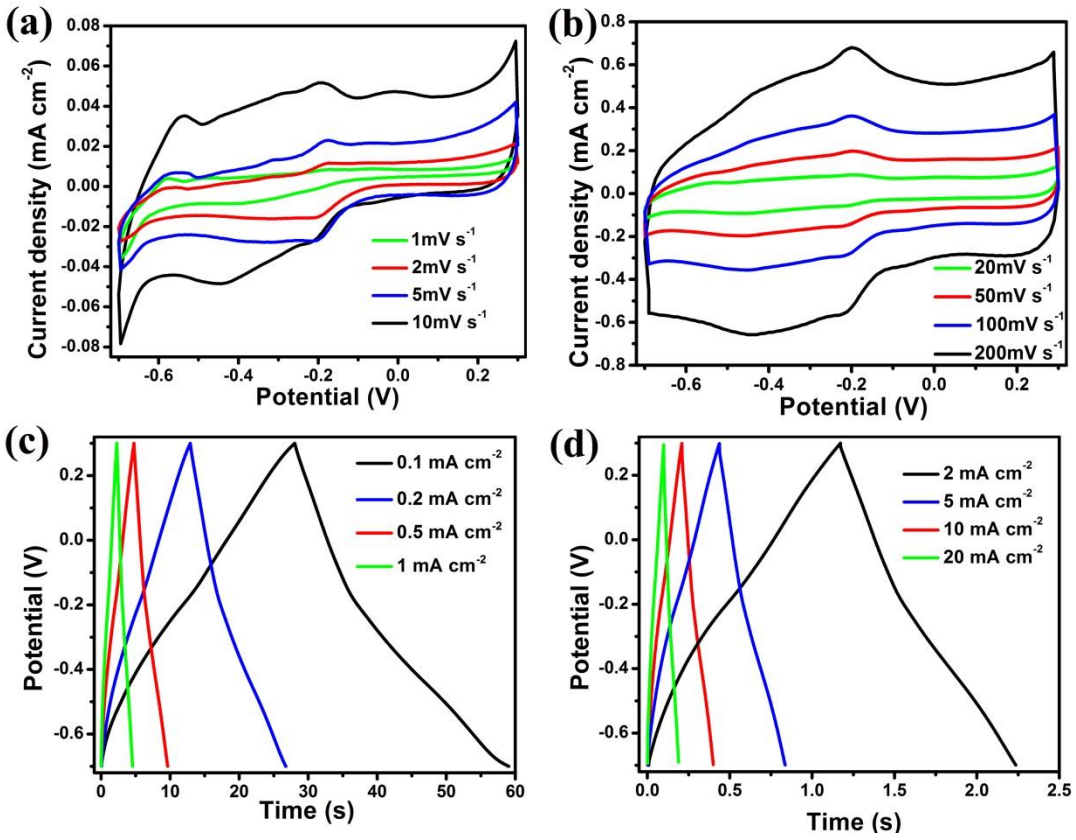

Figure S12. Electrochemical performance of CF electrode tested in three-electrode mode. CV profiles at the scan rates ranging from (a) 1 to 10 mV s^{-1} and (b) 20 to 200 mV s^{-1}. Corresponding GCD curves, operated with current densities ranging from 0.1 to 1 mA cm^{-2} (c) and from 2 to 20 mA cm^{-2} (d).

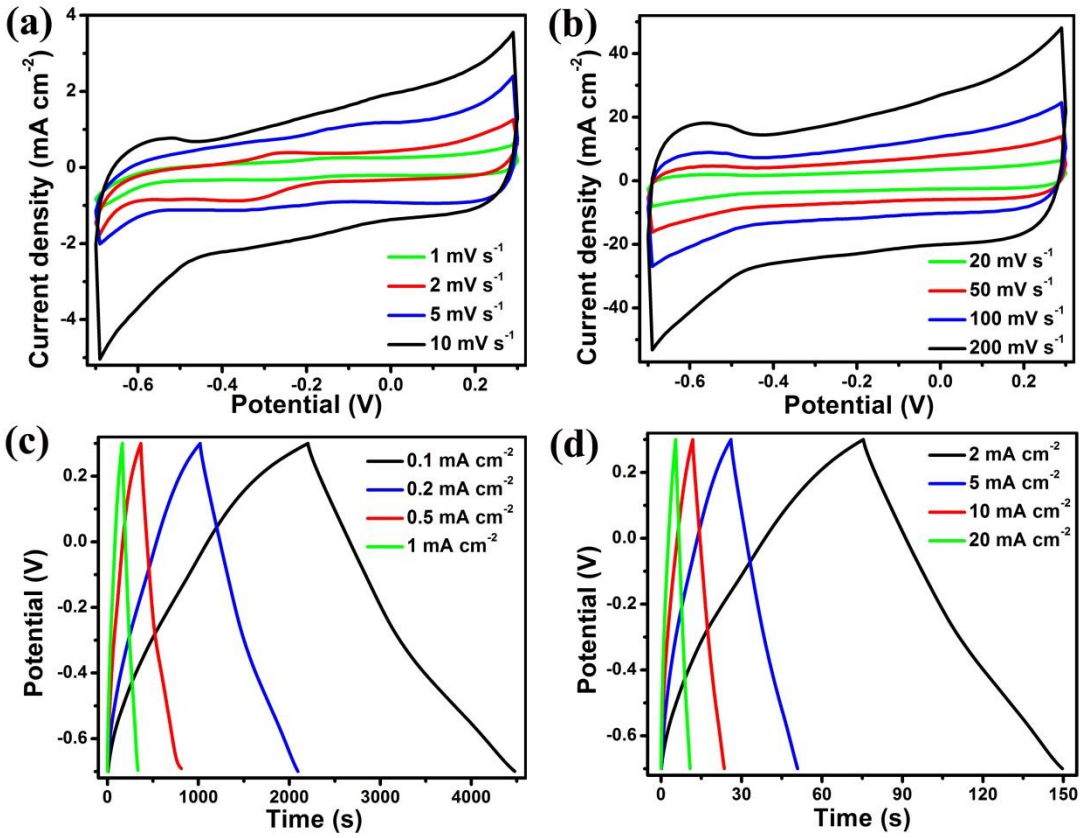

Figure S13. Electrochemical performance of GaN electrode tested in three-electrode mode. CV profiles at the scan rates ranging from (a) 1 to 10 mV s^{-1} and (b) 20 to 200 mV s^{-1}. Corresponding GCD curves, operated with current densities ranging from 0.1 to 1 mA cm^{-2} (c) and from 2 to 20 mA cm^{-2} (d).

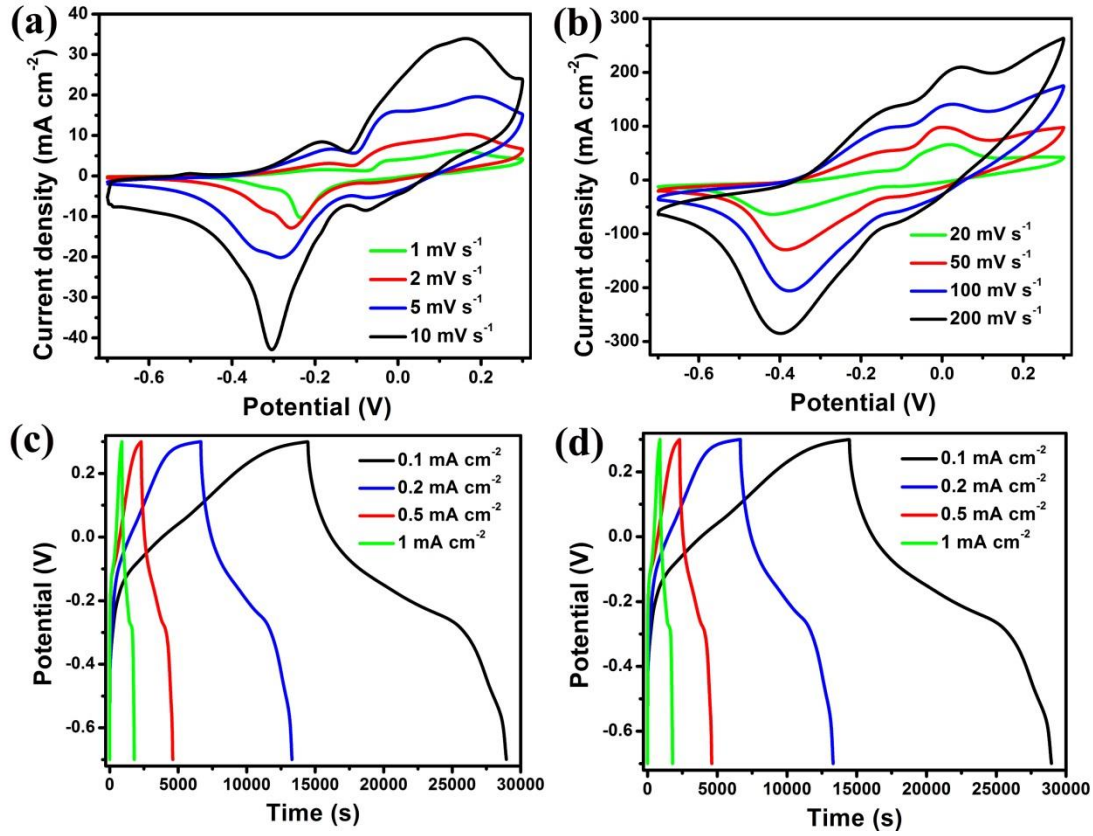

Figure S14. Electrochemical performance of MnO_2 electrode tested in three-electrode mode. CV profiles at the scan rates ranging from (a) 1 to 10 mV s^{-1} and (b) 20 to 200 mV s^{-1}. Corresponding GCD curves, operated with current densities ranging from 0.1 to 1 mA cm^{-2} (c) and from 2 to 20 mA cm^{-2} (d).

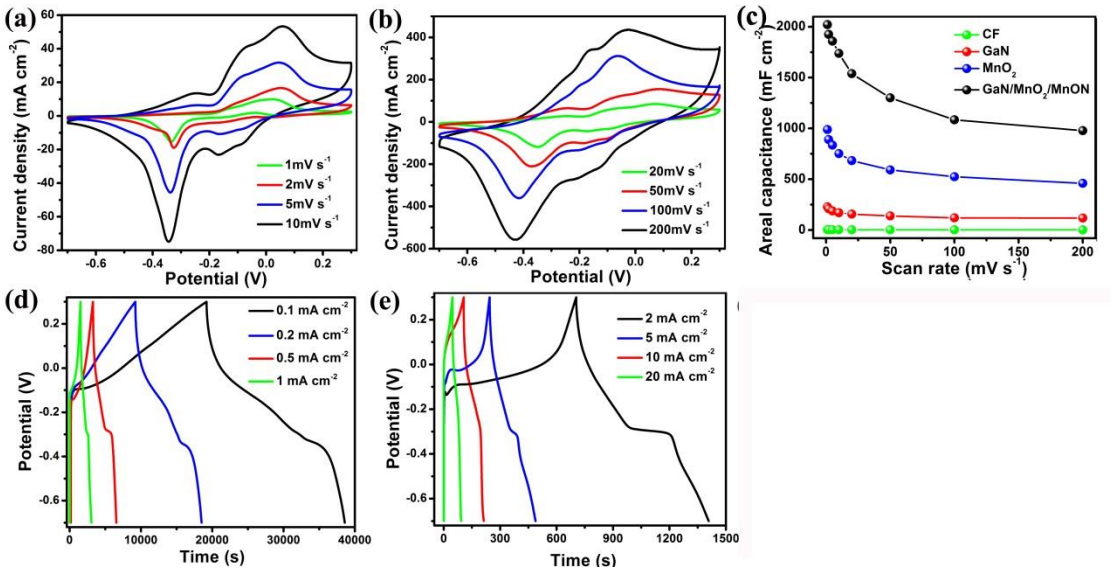

Figure S15. Electrochemical performance of GaN/MnO_2/MnON electrode tested in three-electrode mode. CV profiles at the scan rates ranging from (a) 1 to 10 mV s^{-1} and (b) 20 to 200 mV s^{-1}. (c) The areal specific capacitances of the CF based electrodes as a function of scan rate. Corresponding GCD curves, operated with current densities ranging from 0.1 to 1 mA cm^{-2} (d) and from 2 to 20 mA cm^{-2} (e).

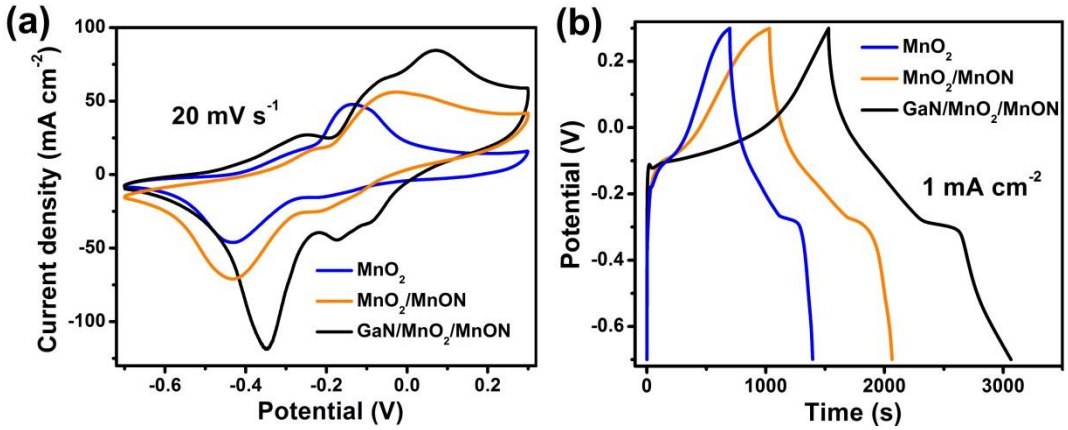

Figure S16. Electrochemical performance comparison of MnO_2, MnO_2/MnON and GaN/MnO_2/MnON, CV curves (a) at 20 mV s^{-1} and GCD curves (b) at 1 mA cm^{-2}.

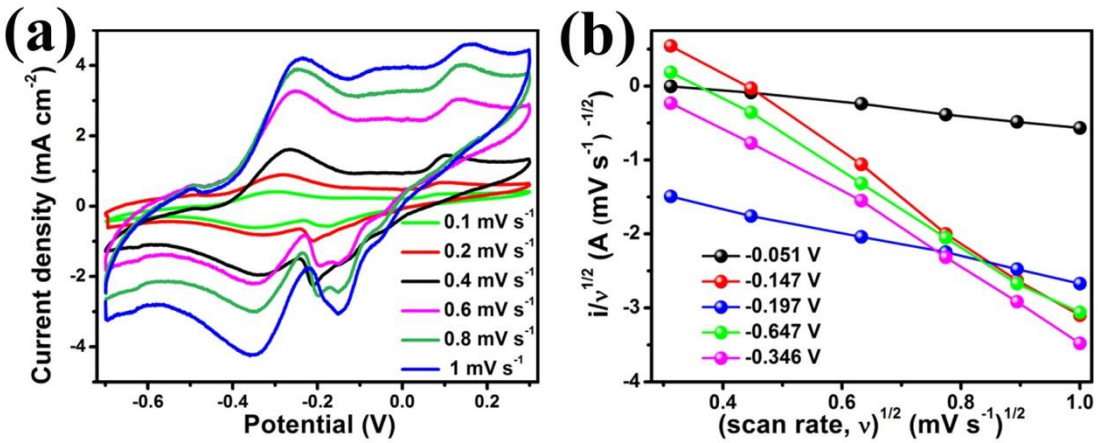

Figure S17. (a) CV curves at different scan rates of the GaN/MnO_2/MnON electrode. (b) Plots of $\nu^{1/2}$ vs. $i/\nu^{1/2}$ used for calculating constants k_1 and K_2 at different potentials.

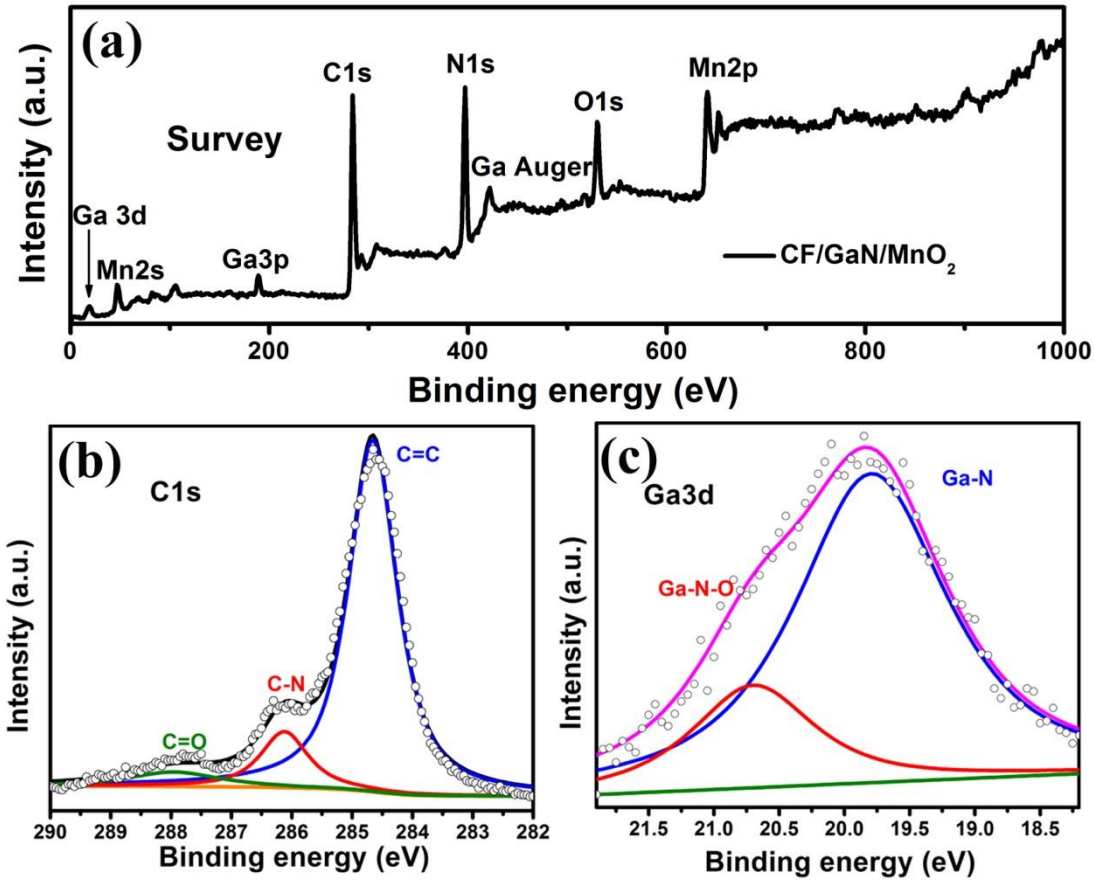

Figure S18. The survey (a), C1s (b), and Ga3d (c) XPS spectra of GaN/MnO_2/MnON electrode.

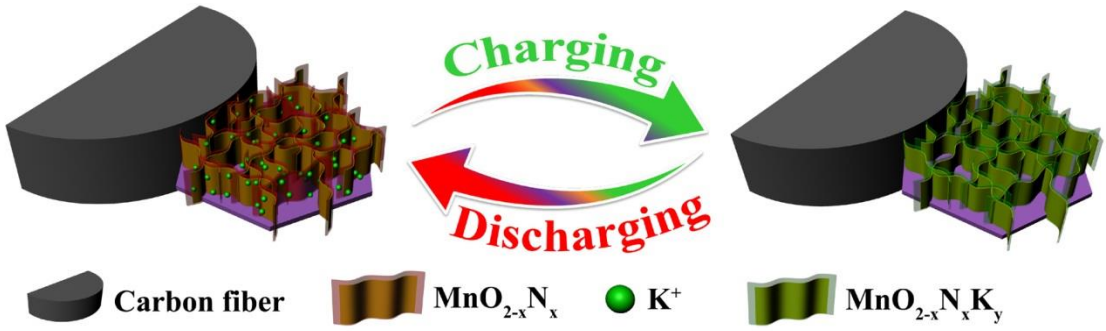

Figure S19. Proposed pseudocapacitive mechanism for charging and discharging of the GaN/MnO_2/MnON electrodes.

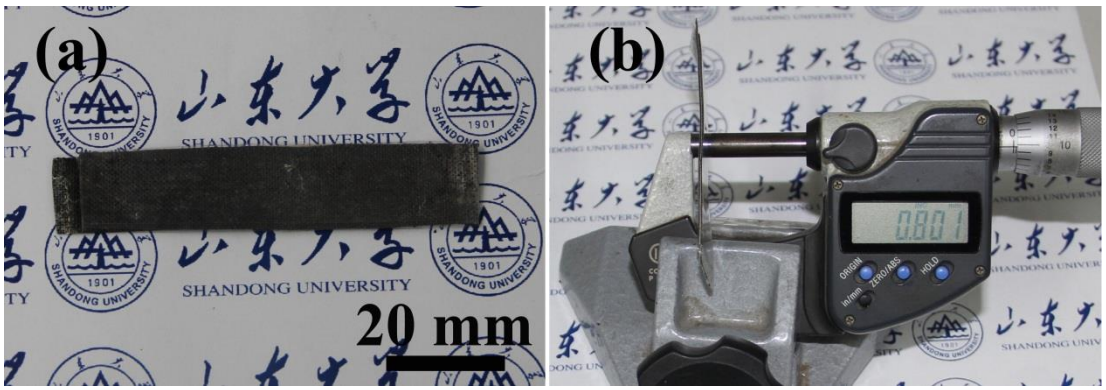

Figure S20. The as-prepared flexible SCs (a) and its thickness (b).

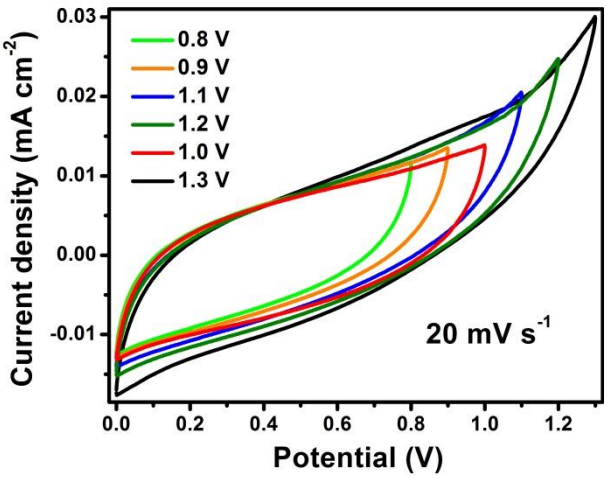

Figure S21. CV curves of the optimized SC device for different scan voltage windows at 20 mV s^{-1}.

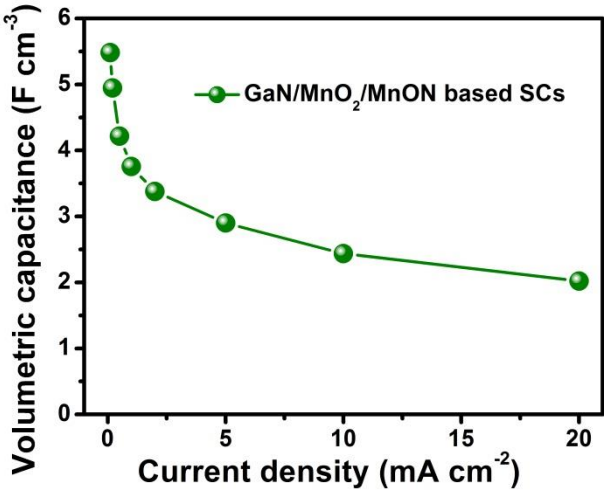

Figure S22. Volumetric capacitances of the flexible SC at different current density.

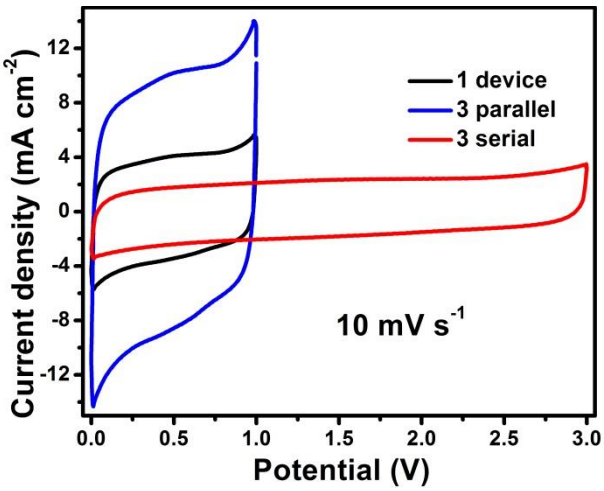

Figure 23. CV curves for SCs with different device configuration at a fixed scan rate of 10 mV s^{-1}.

S7. Table S1–S3

Table S1. The elements content from EDS measurement of GaN/MnO_2/MnON nanocomposite.

Element	Weight%	Atomic%
C K	15.48	27.05
N K	3.77	5.64
O K	39.53	51.82
K K	1.86	1.00
Mn K	32.99	12.58
Ga L	6.37	1.91
Totals	100.00	100.00

Table S2. Fitting report of Figure 5f based on a R(C(RW))C equivalent circuit.

Index	symbol	start	end	% error
1	R1	1.893	1.883	2.45
2	Cdl	0.000034	0.000034	11.2
3	R2	1.187	1.187	4.35
4	W1	0.823	0.828	6.20
5	Cps	1.158	1.156	4.013

Table S3. Comparison of the volumetric power and energy density of the flexible SCs.

Electrodes materials	Energy density mW h cm^{-3}	Power density mW cm^{-3}	window (V)	References
CF/GaN/MnO_2	0.76	125	1.0	this work
CF@CoP	0.69	114.20	1.6	*ACS Appl. Mater. Interfaces*, 2017, **9,** 16986.[15]
TiN-based SSCs	0.045	200	1.0	*Nano Lett.*, 2012, **12,** 5376.[16]
MnO_2/Fe_2O_3	0.41	100	1.6	*Adv. Mater.*, 2014, **26,** 3148.[17]
MnO_2/graphene	0.87	9	1.8	*Adv. Mater.*, 2014, **26,** 5869.[18]
CF@VOx/VN	0.61	80	1.8	*Nano Lett.*, 2013, **13,** 2628.[19]
graphene-based SCs	0.06	135	1.0	*ACS Nano*, 2013, **7,** 4042.[20]
TiO_2-MnO_2	0.3	250	1.8	*Adv. Mater.*, 2013, **25,** 267.[21]
CF@MnO_2	0.55	139.1	1.6	*Nano lett.*, 2014, **14,** 731.[22]
CNT/MnO_2	0.45	13.8	0.8	*J. Mater. Chem. A*, 2014, **2,** 17561.[23]
MnO_2/CF	0.12	0.4	0.8	*ACS Nano*, 2012, **6,** 9200.[24]
Gaphite/GaN	0.3	1000	1.0	*Small*, 2017, **13,** 1603330.[10]

Table S4. Comparison of the areal power and energy density of the flexible SCs.

Electrodes materials	Energy density μW h cm^{-2}	Power density mW cm^{-2}	window (V)	References
CF/GaN/MnO_2	61.0	10	1.0	this work
Graphite/GaN	7.4	25	1	*Small*, 2017, **13,** 1603330.[10]
MnO_2/PEDOT/CNT	96.1	2.7	1.8	*Nano Lett.*, 2017, **17,** 2719.[25]
MnO_2/CF	1.428	0.05	1.5	*Adv. Energy Mater.*, 2016, **6,** 1501458.[26]
MnO_2/GN	8.2	0.93		*J. Mater. Chem. A*, 2014, **2,** 9736.[27]
GN based SC	17.5	0.82		*Nanoscale*, 2015, **7,** 9399.[28]
GN@MnO_2	0.074	0.4		*Nat. Commun.*, 2013, **4,** 2487.[29]
Pours GaN films	0.65	45	0.9	*Adv. Mater.*, 2016, **28,** 3768.[8]
N-SiC	0.12	72.3	0.8	*ACS Nano*, 2015, **9,** 8054.[30]
ZnO	0.015	0.28		*Phys. Chem. Chem. Phys.*, 2013 **15,** 17752.[31]
RGO/PPy	61.4	10	1.0	*J. Power Sources*, 2016, **302,** 39.[32]

References

1. Y. Cui and C. M. Lieber, *Science*, 2001, **291,** 851.
2. P. Simon and Y. Gogotsi, *Nat. Mater.*, 2008, **7,** 845.
3. X. Xiao, X. Peng, H. Jin, T. Li, C. Zhang, B. Gao, B. Hu, K. Huo and J. Zhou, *Adv. Mater.*, 2013, **25,** 5091.
4. Y.-J. B. Ting, K. Lian and N. Kherani, *ECS Trans.*, 2011, **35,** 133.
5. P. Yang, X. Xiao, Y. Li, Y. Ding, P. Qiang, X. Tan, W. Mai, Z. Lin, W. Wu, T. Li, H. Jin, P. Liu, J. Zhou, C. P. Wong and Z. L. Wang, *ACS Nano*, 2013, **7,** 2617.
6. Y. Yoon, K. Lee, C. Baik, H. Yoo, M. Min, Y. Park, S. M. Lee and H. Lee, *Adv. Mater.*, 2013, **25,** 4437.

7. F. Su, J. Zeng, X. Bao, Y. Yu, J. Y. Lee and X. S. Zhao, *Chem.Mate.,* 2005, **17,** 3960.
8. S. Wang, L. Zhang, C. Sun, Y. Shao, Y. Wu, J. Lv and X. Hao, *Adv. Mater.,* 2016, **28,** 3768.
9. X. Xiao, H. Yu, H. Jin, M. Wu, Y. Fang, J. Sun, Z. Hu, T. Li, J. Wu, L. Huang, Y. Gogotsi and J. Zhou, *ACS Nano,* 2017, **11,** 2180.
10. S. Wang, C. Sun, Y. Shao, Y. Wu, L. Zhang and X. Hao, *Small*, 2017, **13,** 1603330.
11. X. Wang, G. Li, Z. Chen, V. Augustyn, X. Ma, G. Wang and B. Dunn, Y. *Adv. Energy Mater.,* 2011, **1,** 1089.
12. J. Wang, J. Polleux, J. Lim and B. Dunn, *J. Phys. Chem. C,* 2007, **111,** 14925.
13. T. Brezesinski, J. Wang, S. H. Tolbert and B. Dunn, *Nat. Mater.*, 2010, **9,** 146.
14. B. Shen, R. Guo, J. Lang, L. Liu, L. Liu and X. Yan, *J. Mater. Chem. A,* 2016, **4,** 8316.
15. Z. Zheng, M. Retana, X. Hu, R. Luna, Y. H. Ikuhara and W. Zhou, *ACS Appl. Mater. Interfaces*, 2017, **9,** 16986.
16. X. Lu, G. Wang, T. Zhai, M. Yu, S. Xie, Y. Ling, C. Liang, Y. Tong and Y. Li, *Nano Lett.,* 2012, **12,** 5376.
17. X. Lu, Y. Zeng, M. Yu, T. Zhai, C. Liang, S. Xie, M.-S. Balogun and Y. Tong, *Adv. Mater.,* 2014, **26,** 3148.
18. T. Zhai, X. Lu, Y. Ling, M. Yu, G. Wang, T. Liu, C. Liang, Y. Tong and Y. Li, *Adv. Mater.,* 2014, **26,** 5869.
19. X. Lu, M. Yu, T. Zhai, G. Wang, S. Xie, T. Liu, C. Liang, Y. Tong and Y. Li, *Nano Lett.,* 2013, **13,** 2628.
20. Y. Xu, Z. Lin, X. Huang, Y. Liu, Y. Huang and X. Duan, *ACS Nano,* 2013, **7,** 4042.
21. X. Lu, M. Yu, G. Wang, T. Zhai, S. Xie, Y. Ling, Y. Tong and Y. Li, *Adv. Mater.,* 2013, **25,** 267.
22. P. Yang, Y. Ding, Z. Lin, Z. Chen, Y. Li, P. Qiang, M. Ebrahimi, W. Mai, C. P. Wong and Z. L. Wang, *Nano lett.,* 2014, 14, 731.

23. L. Du, P. Yang, X. Yu, P. Liu, J. Song and W. Mai, *J. Mater. Chem. A*, 2014, **2,** 17561.
24. X Xiao, T Li, P Yang, Y Gao, H Jin, W Ni, W Zhan, X. Zhang, Y. Cao, J. Zhong, L. Gong, W.-C. Yen, W. Mai, J. Chen, K. Huo, Y.-L. Chueh, Z. L. Wang and J. Zhou, *ACS Nano*, 2012, **6,** 9200.
25. Q Zhang, X Wang, Z Pan, J Sun, J Zhao, J Zhang, C. Zhang, L. Tang, J. Luo, B. Song, Z. Zhang, W. Lu, Q. Li, Y. Zhang and Y. Yao, *Nano Lett.*, 2017, **17,** 2719.
26. N. Yu, H. Yin, W. Zhang, Y. Liu, Z. Tang and M. Q. Zhu, *Adv. Energy Mater.*, 2016, **6,** 1501458.
27. B Zheng, T Huang, L Kou, X Zhao, K. Gopalsamy and C. Gao, *J. Mater. Chem. A*, 2014, **2,** 9736.
28. X Zhao, B Zheng, T Huang and C Gao, *Nanoscale*, 2015, **7,** 9399.
29. Z. S. Wu, K. Parvez, X. Feng and K. Müllen, *Nat. Commun.*, 2013, **4,** 2487.
30. Y. Chen, X. Zhang and Z. Xie, *ACS Nano*, 2015, **9,** 8054.
31. X Li, T Zhao, Q Chen, P Li, K Wang, M. Zhong, J. Wei, D. Wu, B. Wei and H. Zhu, *Phys. Chem. Chem. Phys.*, 2013, **15,** 17752.
32. C Yang, L Zhang, N Hu, Z Yang, H Wei and Y. Zhang, *J. Power Sources*, 2016, **302,** 39.